

PREDICTION OF THE FLOW REGIME IN LIQUID-GAS FLOWS THROUGH STRAIGHT PIPES USING COMPUTATIONAL FLUID DYNAMICS

Ezequiel A. Krumrick^a, Ezequiel J. López^b and Alberto G. Camacho^c

^a*Dpto. de Ingeniería Química, Universidad Tecnológica Nacional, Facultad Regional del Neuquén, Campamento Uno, 8318 Plaza Huincul, Argentina
ekrumrick@yahoo.com.ar*

^b*Dpto. de Mecánica Aplicada, Facultad de Ingeniería, Universidad Nacional del Comahue, CONICET, Buenos Aires 1400, 8300 Neuquén, Argentina
ezequiel.lopez@fain.uncoma.edu.ar*

^c*Director Dpto. de Ingeniería Química, Universidad Tecnológica Nacional, Facultad Regional del Neuquén, Campamento Uno, 8318 Plaza Huincul, Argentina
acamacho@frn.utn.edu.ar*

Keywords: Multiphase flow in pipes, flow regime map, oil-gas flow, Volume of Fluid method, OpenFOAM(R).

Abstract. The simulation of multiphase flows generally relies on the *a priori* knowledge of the flow regime that develops in the problem of interest. In the case of two-phase flow in pipes, this knowledge comes from flow regime maps, which were constructed in the classical literature using both theoretical and experimental basis. Some efforts aiming the construction of those kind of maps were done applying CFD (Computational Fluid Dynamics) tools but to a limited extent. The objective of this study is to use CFD tools in order to examine the behavior of two-phase liquid-gas flow in straight pipes and to capture the corresponding flow regime according to the inlet conditions. In particular, oil-gas flows were considered. These flows were assumed as incompressible and isothermal. The computations were performed for two-dimensional (2D) channels and three-dimensional (3D) pipes, and the results were compared to the flow regime maps available in the literature. A detailed comparison between three- and two-dimensional solutions obtained for the same set of parameters was performed in order to validate the use of 2D simulations for the prediction of the flow regime. The method used to determine the phase boundaries is Volume of Fluid (VOF) and turbulence was treated with the k-epsilon model, as incorporated in the open-source toolkit OpenFOAM(R). Adaptive refinement was applied in order to sharpen the liquid-gas interphase with the aim to reduce the computational cost of the simulations maintaining the total number of cells in a tractable amount. Due to limitations in the mesh size, only a portion of the flow regime map could be assessed, including those flow regimes with features of the interphase captured by the mesh. These results were compared with the flow regime map of Taitel and Dukler and other maps constructed from experimental results, where the emphasis was put in the limits defining regions inside the map.

1 INTRODUCTION

Simultaneous gas and liquid flow is a very common phenomenon in the chemical and oil industries, particularly in transportation lines and process equipment. For this reason, the study of the characteristics and mechanisms of two-phase and multiphase flow has generated great interest, especially in the oil industry, where the possibility of transportation of gas, oil and water from the field to the processing plant in a single pipe, results in a considerable reduction of costs.

For the design of these pipes, it is required to estimate the pressure drop as precisely as possible. The dimensioning of transmission lines with multiphase flow requires additional or different criteria as those used for the design of single-phase lines. Unlike with single-phase lines, oversizing a line with multiphase flow can cause serious problems.

Flow assurance is essential for the transport of multiphase fluids and requires assessments on both, steady state and dynamic simulations, that establish possible complications that may arise in the system, resulting from disturbances that generate changes in flow regimes along the system.

Many efforts have been made to identify the flow pattern developed by the stream of a liquid and a gas in a pipe. The first and may be most widely known theoretical work was the [Taitel and Dukler \(1976\)](#) map, which has served as a kick start for other researchers of this line of investigation. Other researchers have focused in empirical maps, one of which is the Beggs and Brill map ([Beggs et al., 1973](#)). The most recent development in mechanistic models, at least as known by the authors of these lines, is the work by [Petalas et al. \(2000\)](#), which makes some improvements to the work by [Taitel and Dukler \(1976\)](#) and other authors, taking into account, for example, the rugosity of the pipe wall and the interfacial friction.

Due to the relatively high cost and practical limitations of a physical installation to analyse the behaviour of gas-liquid mixtures, in recent years, there has been a crescent interest in computer simulation of multiphase flow. Some of the last developments on this topic are the works by [Shuard et al. \(2016\)](#), [Min \(2015\)](#), [Thaker and Banerjee \(2013\)](#), [Vershinin et al. \(2015\)](#) and [Izarra Labeaga and Herreras Omagogeascoa \(2013\)](#), among others. These researchers have focused on different issues of numerical simulation of two-phase flow. Izarra Labeaga and Vershinin did their simulations in two-dimensions (2D), while Lu, Thaker and Shuard did theirs in three-dimensions (3D).

The objective of the present work is to provide both, a new focus to two-phase simulation utilising dynamic mesh refinement and a comparison between 2D and 3D simulations for a wide range of combinations of gas-liquid flow. A total of seventeen simulations were carried out for 2D channels and fourteen of these cases were replicated for 3D half pipes, where the Navier-Stokes equations were solved assuming incompressible isothermal flow for two immiscible fluids. The method used to determine the phase boundaries is Volume of Fluid (VOF) and turbulence was treated with the standard $k - \epsilon$ model ([Wilcox, 2006](#)), as incorporated in the open-source toolkit OpenFOAM®. Adaptive mesh refinement was applied in order to sharpen the liquid-gas interphase with the aim to reduce the computational cost of the simulations maintaining the total number of cells in a tractable amount. Due to limitations in the mesh size, only a portion of the flow regime map could be assessed, including those flow regimes with features of the interphase captured by the mesh. The results obtained in the simulations were then compared with a flow regime map based on the mechanistic model by [Petalas et al. \(2000\)](#).

2 CHARACTERISTIC TWO-PHASE FLOW IN HORIZONTAL PIPES

Figure 1 shows the general types of visualization generated in this analysis: stratified smooth, stratified wavy, dispersed bubble, slug and froth flow (Crowe, 2005). The following subsections give the commonly accepted characterization of these regime flows.

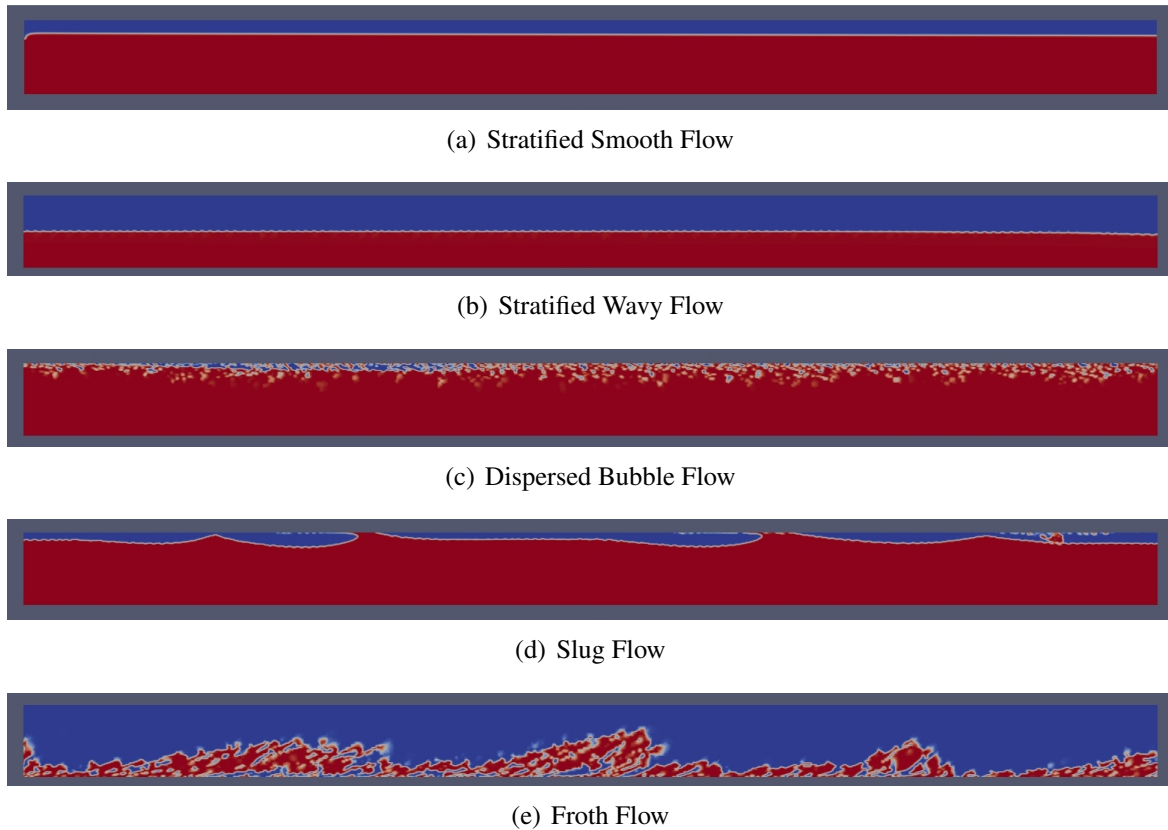


Figure 1: Characteristic two-phase flow analyzed in this work. The red color represents liquid and the blue color represents gas.

2.1 Stratified flow

Stratified flow is a multiphase flow regime in which fluids are separated into different layers, with lighter fluids flowing above heavier fluids. Stratified flow is more likely to occur at low flow rates and in flat or downhill sections of horizontal wells. If the flow rates of the fluids are sufficiently low, the interface between them remains stable, and the flow is known as stratified smooth (SS), but as the flow rate increases, the interface becomes mixed and irregular, and the flow is named stratified wavy (SW).

2.2 Dispersed bubble flow

Dispersed bubble flow (DB) is a multiphase flow regime in which one fluid moves as small dispersed bubbles, through a continuous fluid. The relative velocity of the bubbles depends essentially on the difference in density between the two fluids. Bubble flow usually occurs at low flow rate and low holdup of the bubbly fluid. As the velocity of the continuous fluid increases, the bubbles are dispersed into smaller, more separated bubbles.

2.3 Elongated bubble flow

Elongated bubble flow (EB) is a multiphase flow regime in which most of the gas, moves as large bubbles dispersed within a continuous liquid. The bubbles may cross much of the pipe. There are also small bubbles within the liquid, but many of these have coalesced to form the larger bubbles or plugs. Elongated bubble flow is similar to slug flow, but the bubbles are smaller and move slower.

2.4 Slug flow

Slug flow (SL) is a multiphase flow regime in which most of the lighter fluid is contained in large bubbles dispersed within, and pushing along the heavier fluid. Slug normally refers to the heavier, slower moving fluid. There are also small bubbles within the liquid, but many of these have coalesced to form the large bubbles until they span much of the pipe. In gas-liquid mixtures, slug flow is similar to elongated bubble flow, but the bubbles are generally larger and move faster.

2.5 Annular mist flow

Annular mist (AM) is a multiphase flow regime in which the lighter fluid flows in the center of the pipe and the heavier fluid is contained in a thin film on the pipe wall. Annular flow occurs at high velocities of the lighter fluid. As the velocity increases, the film may disappear, leading to mist flow.

2.6 Froth flow

Froth flow (F) is a transition between other well defined multiphase flow regimes, such as between stratified and annular, or as between slug and annular flows.

3 NUMERICAL APPROACH

3.1 OpenFOAM

OpenFOAM® (Open-source Field Operation and Manipulation) is an open-source C++ library used to create executable applications, consisting of solvers and utilities, designed primarily around three-dimensional continuum mechanics. It also includes pre and post-processing utilities. The overall structure of the toolkit is shown in Fig. 2 (<http://www.openfoam.org>).

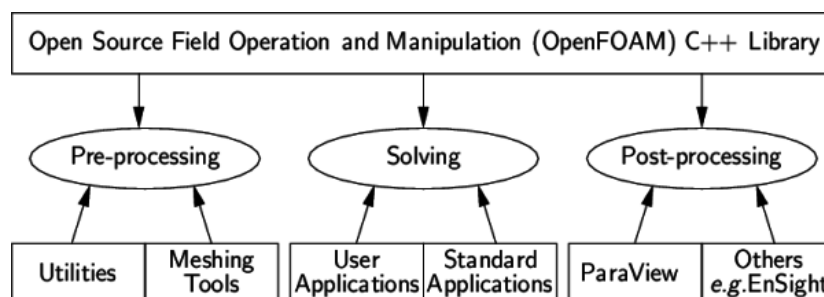


Figure 2: Overall structure of OpenFOAM®.

OpenFOAM's solvers utilize the finite volume method with a co-located methodology on an unstructured polyhedral grid with arbitrary grid elements.

3.2 The interFoam solver

InterFoam implements a Volume of Fluid (VOF) algorithm for multiphase flow. It includes the multidimensional limiter for an explicit solution (MULES) as a method of guaranteeing boundedness of scalar fields, in particular phase/mass-fractions. An additional artificial compression term is activated in the phase-fraction equation as shown in the third term of Eqn. (1).

$$\frac{\partial \alpha_a}{\partial t} + \nabla \cdot (\mathbf{U} \alpha_a) + \nabla \cdot (\mathbf{U}_r \alpha_a (1 - \alpha_a)) = 0 \quad (1)$$

In the above equation α_a is the phase fraction, t is time and \mathbf{U} is the phase velocity. The compression term works only in the thin interface region including a compression velocity \mathbf{U}_r which operates in the perpendicular direction to the interface. This compression velocity is based on the velocity magnitude in the transition region. The maximum velocity magnitude U_{max} is multiplied by the normal vector to the interface and an adjustable coefficient K_c defining the extent of the compression as shown in Eqn. (2) (Hänsch et al., 2013).

$$\mathbf{U}_r = K_c U_{max} \frac{\nabla \alpha_a}{|\nabla \alpha_a|} \quad (2)$$

3.3 The interDyMFoam solver

The interDyMFoam solver is a variation of the interFoam solver with optional mesh motion and mesh topology changes including adaptive re-meshing. It offers the possibility of utilizing a coarse mesh with refinement in the areas of interest, in this case, the interphase, reducing the computational times notably with a small sacrifice in accuracy.

4 PROBLEM SETUP

The problem consists in a horizontal straight pipe inside of which flows a stream of gas and oil with different superficial velocities. The superficial velocity is defined as the velocity at which each phase would flow if it spans the whole pipe cross-section keeping the volumetric flow of the multiphase case. The pipe diameter is 0.08 m. Pipe wall was considered smooth and the influence of rugosity was neglected in order to simplify the numerical study. The gravitational acceleration was applied in the normal direction to the pipe axis.

The physical properties of the fluids in which the simulations were based are described in Table 1.

| Parameter | Value | Units |
|-------------------------|-----------------------|-------------------|
| Gas density | 12 | kg/m ³ |
| Oil density | 820 | kg/m ³ |
| Gas kinematic viscosity | 1.48×10^{-5} | m ² /s |
| Oil kinematic viscosity | 4×10^{-5} | m ² /s |
| Interfacial tension | 7×10^{-2} | N/m |

Table 1: Physical properties of fluids considered in the simulations.

4.1 Mechanistic flow pattern map

The combination of different superficial velocities of gas and oil, results in a specific flow pattern map, ranging from Stratified Smooth to Annular Mist and Dispersed Bubble for the

data selected in this work. The map is also a function of the physical properties of the fluids involved.

Scilab 5.5.2 was employed to develop a script based on the Petalas and Aziz mechanistic model, where the corresponding map for the particular conditions given above could be appreciated in Fig. 3. In the figure, V_{SG} is the gas superficial velocity and V_{SL} represents the liquid superficial velocity. The map is marked with red dots to indicate the simulated cases.

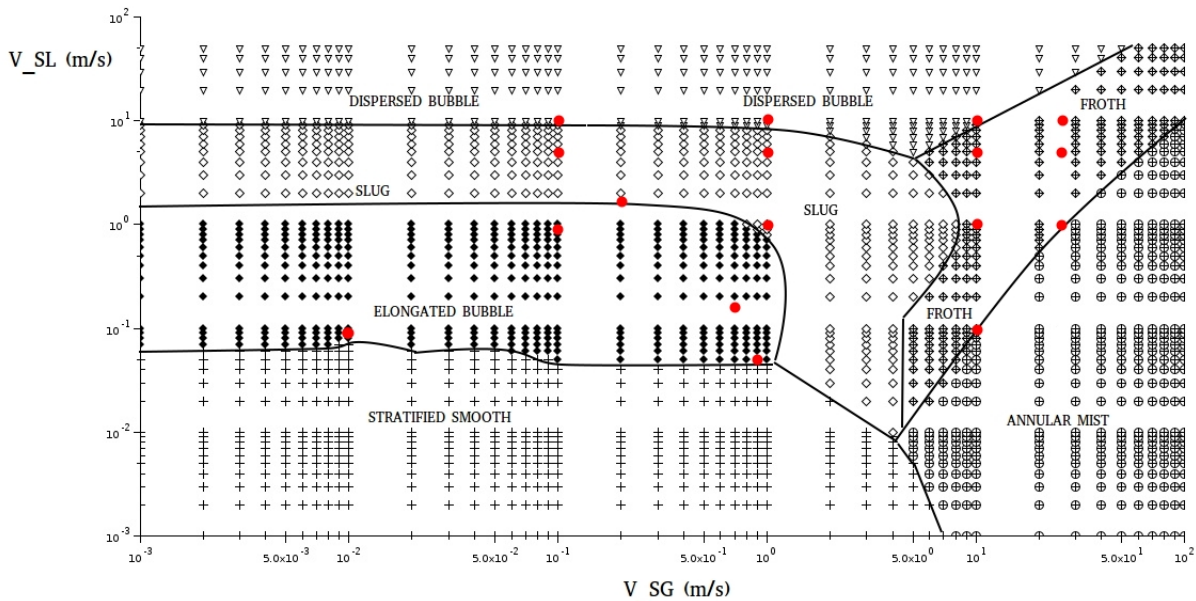


Figure 3: Mechanistic flow pattern map based on the Petalas and Aziz model. The red dots indicate the cases simulated in the present work.

4.2 Configuration of the CFD simulations

OpenFOAM 3.0.1 was employed to simulate the cases using the interFoam and interDyM-Foam solvers. As a first approach to the problem, the turbulence was modeled with the standard $k - \epsilon$ model. It is known that no single turbulence model can be employed in the whole range of turbulent states encountered in multiphase flows (Yeoh and Tu, 2010), especially in the present study where several regime flows are expected to be observed in the simulations. The use of others turbulence models and its performance comparison deserves further analysis beyond the objectives of the present article due to the large computational work involved.

The pipe was simulated considering both 2D and 3D domains, where these domains were defined with the same hydraulic diameter of 0.08 m. Therefore, the 2D domain is a channel 0.04 m in height and 5 m in length and it was discretized using a structured mesh composed of 162000 cells. This mesh was generated using the blockMesh utility provided with OpenFOAM®. Each 2D case was simulated firstly with a relatively coarse mesh, with squared cells with a side length of 1.8 mm. Then, this mesh was uniformly refined in order to obtain a finer mesh with cells sized 1.11 mm. The improvement in the results was evident, as flow patterns could be better identified after refinement. No further refinement was made as the resources required for this simulations were notably increased.

For the 3D domain, only half-pipe was considered assuming symmetry of the flow with respect to the middle vertical plane of the pipe with the aim to reduce the computational cost. The 3D half-pipe was constructed with a diameter of 0.08 m and a length of 5 m and was discretized with a base mesh of 143000 hexahedral cells before dynamic refinement. This base grid was generated with the blockMesh utility as incorporated in OpenFOAM®. Figure 4 shows this mesh in the pipe cross-section.

The initial 3D mesh is relatively coarse but, after achieving an almost periodic flow, they were improved utilizing adaptive refinement, up to two levels. The refinement was performed only considering the oil-gas interphase. Although this was sufficient in many cases to obtain a visually defined flow, it was not enough to get reliable pressure drops compared to the mechanistic model of Petalas and Aziz, since no further flow features were accounted for. The coarser initial mesh of the half cylinder had a maximum cubic cell size of approximately 4.44 mm. After two successive refinements, the maximum cell size was reduced to 1.11 mm near the oil-gas interface.

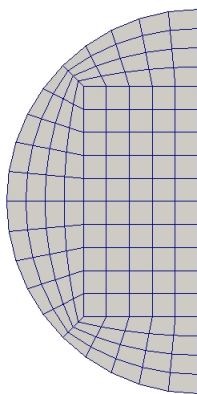


Figure 4: Base grid of the 3D half-pipe.

The mean Courant number was limited to a value of 0.5 and the interface Courant number was also set to 0.5, with this values was possible to achieve the convergence of the solution.

The numerical schemes adopted were the interFoam standards. The convection term in the momentum equation, $\nabla \cdot (\rho \mathbf{U} \mathbf{U})$, denoted by the `div(rho*phi,U)` keyword, uses Gauss linearUpwind grad(U). The $\nabla \cdot (\mathbf{U} \alpha)$ term, represented by the `div(phi,alpha)` keyword uses the vanLeer scheme. The $\nabla \cdot (\mathbf{U}_r \alpha)$ term, represented by the `div(phirb,alpha)` keyword, uses a second order linear differencing.

Calculations for pressure-velocity coupling were performed with the PIMPLE algorithm with three corrector loops and interface compression activated. All simulations were done with a fixed velocity inlet, a zeroGradient condition at the outlet, and “law-of-the-wall” condition at the walls. The dynamic pressure was specified as zeroGradient for both inlet and outlet. The dynamic pressure is represented by p_{rgh} , which means local pressure minus the hydrostatic part. These boundary conditions for both, 2D an 3D cases, are described in Table 2. An initial solution with the potentialFoam solver was required for the 3D cases. Turbulence variables k and ϵ were initialized using typical approximations based on a turbulence intensity and an estimated length scale.

As stated above, the mesh was refined either uniformly (2D cases) or adaptively (3D cases), where in the later cases, cells were refined only considering the oil-gas interphase. This refine-

ment strategy could leads to a coarse mesh in the near-wall region and, thus, an objetable use of “law-of-the-wall” functions. In order to check whether the cell size near walls is suficient to assure a correct application of the “law-of-the-wall” functions, a postprocess analysis was performed where values of the dimensionless distance to the wall y^+ were computed (see section 5, Table 5). This dimensionless distance to the wall is defined as (Wilcox, 2006)

$$y^+ = \frac{u_\tau y}{\nu} \quad (3)$$

where $u_\tau = \sqrt{\tau_w/\rho}$ is the friction velocity, τ_w is wall shear stress, ρ is the density, y is the actual distance to the wall, and ν is the kinematic viscosity.

| Parameter | Inlet | Outlet | Walls |
|-----------|----------------------|----------------------|----------------------|
| U | fixedValue | zeroGradient | fixedValue uniform 0 |
| p_rgh | zeroGradient | zeroGradient | zeroGradient |
| k | fixedValue | zeroGradient | kqRWallFunction |
| nut | Calculated uniform 0 | Calculated uniform 0 | nutkWallFunction |
| epsilon | fixedValue | zeroGradient | epsilonWallFunction |

Table 2: Boundary conditions.

For each case, the simulation time was firstly estimated under the condition that the phase with lower inlet superficial velocity crosses at least once the pipe length as it moves with this velocity. At this “provisory” final time, it was checked if a periodic solution was reached. If not, the simulation was continued until a periodic state, or almost periodic, is obtained. In this way, if the pipe is long enough to develop the corresponding flow pattern, it is expected the simulated flow has sufficient time to evolve. In some cases the assumed pipe length could be insufficient to develop the correct regime flow, but this is unknown *a priori* and due to computational resources reasons, the pipe length was taken as constant.

5 RESULTS

Assuming that multiphase flow is almost periodic, the main characteristics of the different flow patterns could be identified. Table 3 summarizes the results obtained for 2D and 3D simulations flow patterns and its comparison with the mechanistic model of Petalas and Aziz. The length of the pipe was 5 m for most cases, however, periodic flow needs a minimum length and also a minimum grid resolution to develop properly and in some cases this proved insufficient. In general, there was good agreement between the flow patterns calculated with the mechanistic model and the results of the simulations. There were a few cases in which the length of the pipe was probably not sufficient to develop the expected pattern of flow.

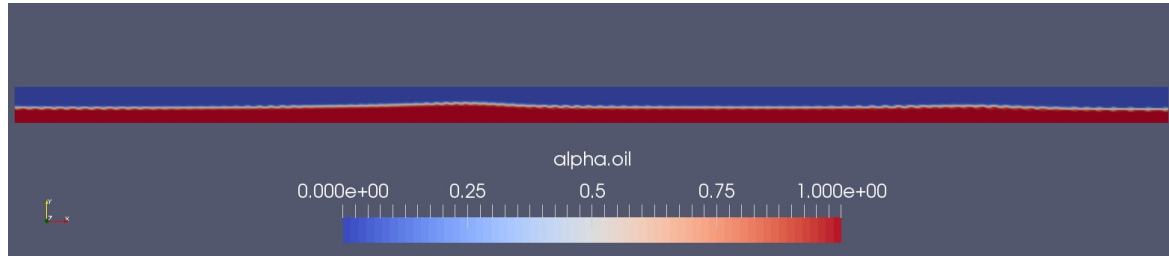
Figure 5 shows the improvement of refining the 2D mesh. In Fig. 5(a) the flow seems to be stratified wavy, while in Fig. 5(b) it is clear that the liquid touches the top of the pipe, and the flow could then be classified as slug or elongated bubble, depending on the periodicity of the slug.

In the case of the 3D simulation for the same conditions, Fig. 6(a) and Fig. 6(b) show the results of one and two levels of refinement. In both of these cases, the resultant flow pattern is stratified wavy.

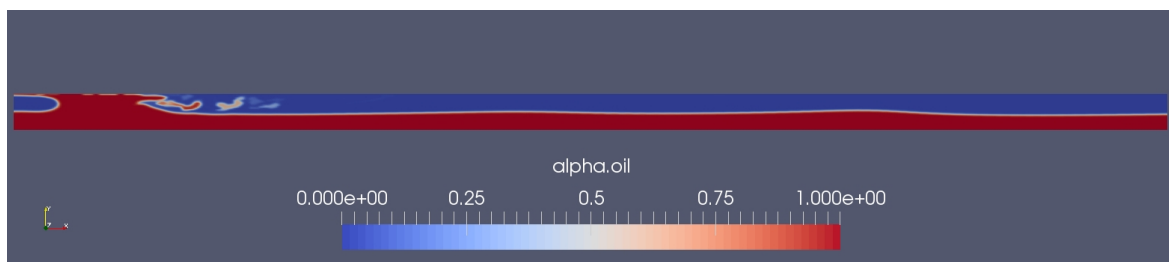
The flow pattern for every case was analyzed by observation of the interface at the symmetry plane of the pipe, like in Fig. 7(a), and also by observation of slices perpendicular to the direction of the flow, like in Fig. 7(b) In these figures flow goes from left to right.

| Case | V_{SG} | V_{SL} | Petalas-Aziz | OF 2D | OF 3D |
|------|----------|----------|--------------|-------|-------|
| 1 | 0.01 | 0.09 | EB | SS | SS |
| 2 | 0.1 | 0.9 | EB | EB | SS |
| 3 | 0.1 | 5 | SL | DB | DB |
| 4 | 0.1 | 10 | DB | DB | — |
| 5 | 0.2 | 1.8 | SL | SL | SW |
| 6 | 0.7 | 0.15 | EB | EB | SW |
| 7 | 0.9 | 0.05 | EB | SW | — |
| 8 | 1 | 1 | SL | SL | SW |
| 9 | 1 | 5 | SL | SL | SL |
| 10 | 1 | 10 | DB | SL | F |
| 11 | 10 | 0.1 | F | F | F |
| 12 | 10 | 1 | F | F | F |
| 13 | 10 | 5 | F | F | F |
| 14 | 10 | 10 | DB | F | F |
| 15 | 25 | 1 | F | F | F |
| 16 | 25 | 5 | F | F | F |
| 17 | 25 | 10 | F | F | — |

Table 3: Comparison of the flow pattern obtained in the simulated cases with the prediction of the Petalas and Aziz model, DB=Dispersed Bubble; EB=Elongated Bubble; F=Froth; SL=Slug; SS=Stratified Smooth; SW=Stratified Wavy



(a) Coarse mesh

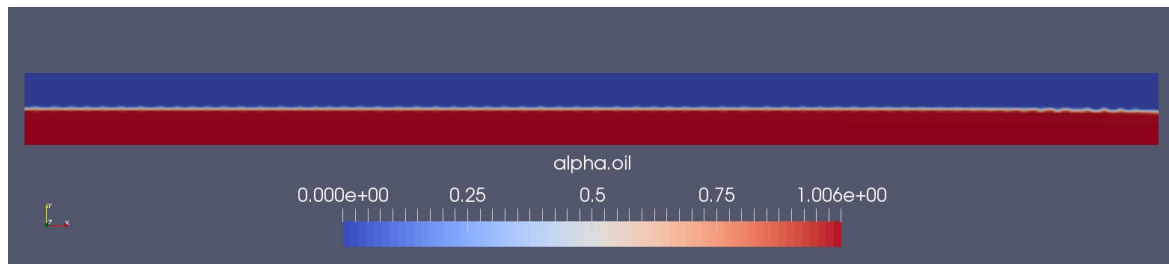


(b) Fine mesh

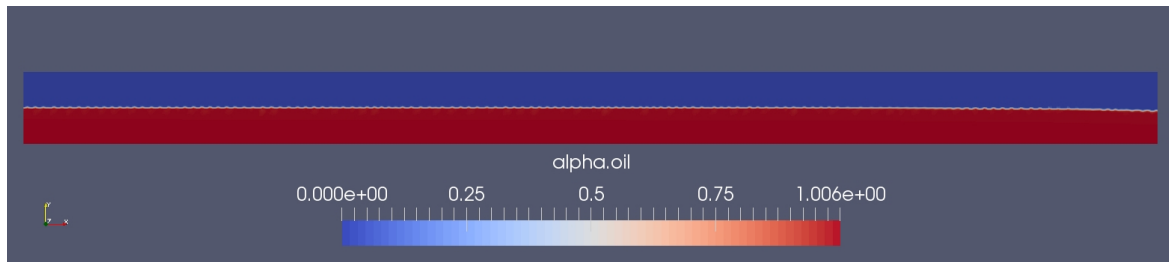
Figure 5: 2D simulation of case $V_{SG}=0.7$ m/s and $V_{SL}=0.15$ m/s with coarse and fine mesh (flow goes from left to right). In this example could be appreciated the different flow pattern obtained after refinement.

Figure 8 shows the topology of the mesh for the case of $V_{SG}=10$ m/s and $V_{SL}=0.1$ m/s after two levels of refinement. In this image, it could be appreciated that the cells that are not involved in the interface, are not refined.

The results of pressure gradient are compared in Table 4. In general, it was found that the



(a) One level of refinement



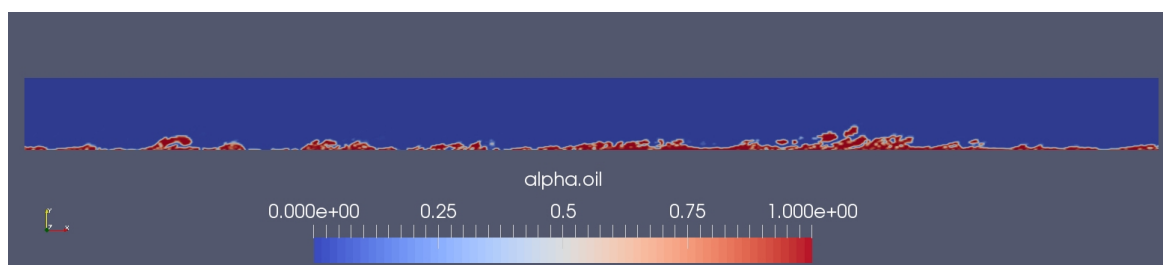
(b) Two levels of refinement

Figure 6: 3D simulation of case $V_{SG}=0.7$ m/s and $V_{SL}=0.15$ m/s with two levels of refinement (flow goes from left to right). In this example could not be appreciated any difference in the flow pattern obtained after refinement.

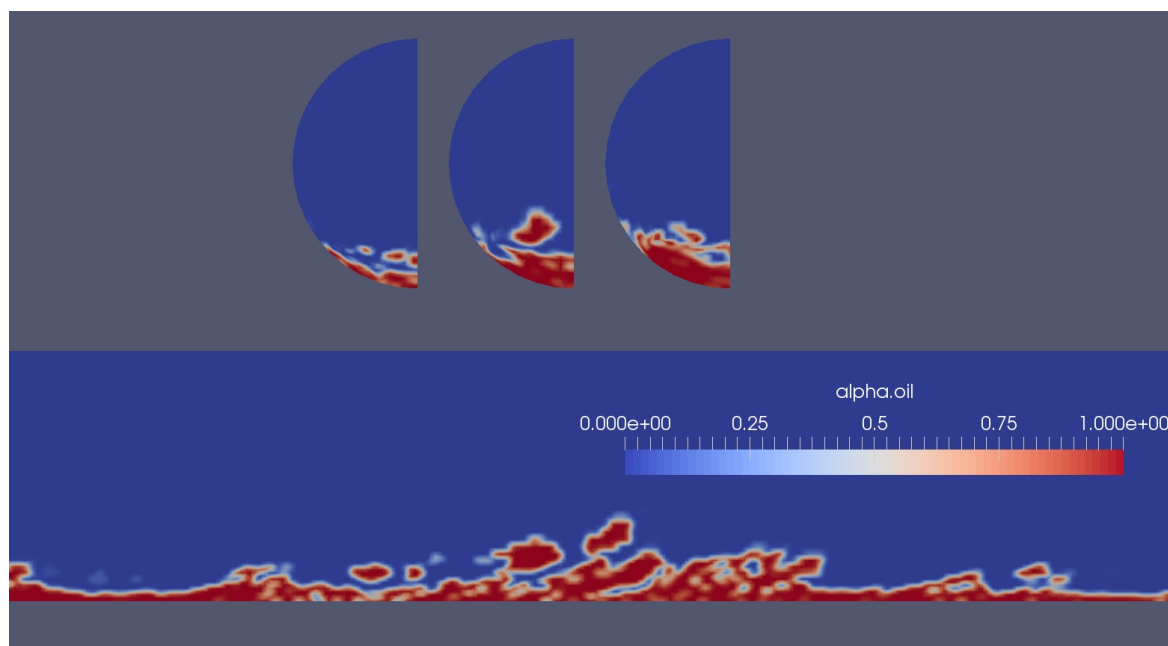
simulation overpredicted by as far as a hundred percent the values of pressure drops when compared with the mechanistic model. The better approximations for pressure drop were obtained for those flows in which the interface proximity to the wall of the pipe was very close, particularly for Froth flow. However, Petalas and Aziz indicated that their model is able to predict pressure drop with an accuracy of 15% for 42% of the cases analyzed by them.

| Case | V_{SG} | V_{SL} | Petalas-Aziz | OF 2D | OF 3D |
|------|----------|----------|--------------|-------|-------|
| 1 | 0.01 | 0.09 | 16 | 17 | 18 |
| 2 | 0.1 | 0.9 | 236 | 410 | 381 |
| 3 | 0.1 | 5 | 3956 | 5662 | 3163 |
| 4 | 0.1 | 10 | 13406 | 5122 | — |
| 5 | 0.2 | 1.8 | 751 | 1173 | 1490 |
| 6 | 0.7 | 0.15 | 105 | 227 | 92 |
| 7 | 0.9 | 0.05 | 68 | 211 | — |
| 8 | 1 | 1 | 543 | 1269 | 1188 |
| 9 | 1 | 5 | 4639 | 5952 | 3770 |
| 10 | 1 | 10 | 14530 | 11232 | 16560 |
| 11 | 10 | 0.1 | 1400 | 1067 | 1040 |
| 12 | 10 | 1 | 3052 | 1624 | 4789 |
| 13 | 10 | 5 | 9583 | 16144 | 14029 |
| 14 | 10 | 10 | 26237 | 20409 | 36864 |
| 15 | 25 | 1 | 2535 | 6888 | 34136 |
| 16 | 25 | 5 | 13996 | 25268 | 39725 |
| 17 | 25 | 10 | 35419 | 54862 | — |

Table 4: Comparison of pressure gradient [Pa/m].



(a) Simmetry plane of pipe



(b) Slices perpendicular to flow direction

Figure 7: Analysis of flow pattern for 3D simulation of case $V_{SG}=10$ m/s and $V_{SL}=0.1$ m/s (flow goes from left to right).

Pressure drop depends strongly on the refinement against the wall of the pipe and the methodology employed here has had poor results regarding this near-wall feature of the flow. In order to get an idea of the refinement level used near the walls in the simulated cases, Table 5 presents typical values of the dimensionless distance to the wall y^+ . A value of y^+ below 100 is, in general, a good estimate to assure that the center of the first cell near the wall falls into the logarithmic layer (Wilcox, 2006), at least in the single-phase case. As expected, y^+ presents greater values for gas than for oil and increases when the superficial velocities augment. For most of 2D cases, typical values of y^+ are below 100. The 3D cases present greater values of y^+ , which reflects the use of a coarser mesh when compared with the 2D mesh. Nevertheless, it is not clear the dependence of mesh refinement near the wall (evaluated via y^+) and the lack of agreement of the computed pressure gradients when compared with the mechanistic model results, since good agreement in the pressure drop was found in some cases with high values of y^+ .

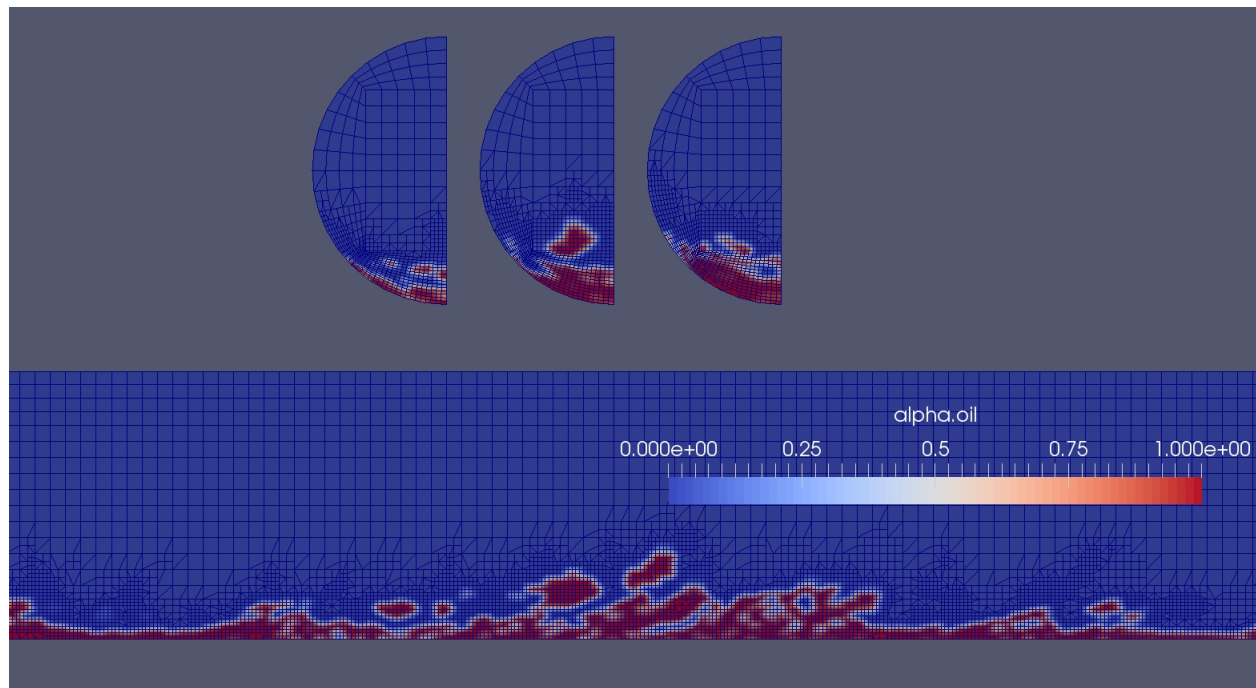


Figure 8: 3D simulation of froth flow with mesh details (flow goes from left to right).

| Case | V_{SG} | V_{SL} | y^+ Gas 2D | y^+ Oil 2D | y^+ Gas 3D | y^+ Oil 3D |
|------|----------|----------|--------------|--------------|--------------|--------------|
| 1 | 0.01 | 0.09 | — | — | 3.88 | 0.84 |
| 2 | 0.1 | 0.9 | 4.15 | 3.42 | 7.74 | 2.16 |
| 3 | 0.1 | 5 | 15.77 | 5.48 | 40.74 | 15.07 |
| 4 | 0.1 | 10 | 23.58 | 8.66 | — | — |
| 5 | 0.2 | 1.8 | 2.32 | 2.69 | 19.44 | 7.52 |
| 6 | 0.7 | 0.15 | 3.27 | 0.17 | 26.95 | 4.48 |
| 7 | 0.9 | 0.05 | 2.91 | 2.03 | — | — |
| 8 | 1 | 1 | 10.34 | 3.82 | 58.18 | 6.89 |
| 9 | 1 | 5 | 7.36 | 5.79 | 63.31 | 15.88 |
| 10 | 1 | 10 | 28.26 | 8.67 | 40.34 | 15.88 |
| 11 | 10 | 0.1 | 26.35 | 10.11 | 99.78 | 8.21 |
| 12 | 10 | 1 | 26.25 | 10.01 | 149.46 | 8.23 |
| 13 | 10 | 5 | 40.18 | 13.70 | 223.11 | 36.67 |
| 14 | 10 | 10 | 46.54 | 14.58 | 323.61 | 46.58 |
| 15 | 25 | 1 | 57.76 | 21.38 | 138.91 | 51.21 |
| 16 | 25 | 5 | 100.78 | 37.29 | 486.15 | 122.43 |
| 17 | 25 | 10 | 112.03 | 29.91 | — | — |

Table 5: Values of y^+ for gas and oil phases in 2D and 3D cases.

6 CONCLUSIONS

Two-phase flows of oil and gas in straight horizontal pipes were simulated using CFD tools with the goal to capture the corresponding flow regime according to the inlet conditions. Simulations were performed with the toolkit OpenFOAM®, and considering the pipe as both, a 2D channel and a 3D half-pipe. Most of the simulated cases showed good visual agreement with the mechanistic model of Petalas and Aziz, however, a few did not coincide, probably, because of a short length assumed for the pipe that resulted insufficient for the proper development of the flow pattern. It was found that for the conditions adopted in this work, two-phase flow could be successfully simulated in 2D channels, with similar results to 3D pipes. In addition, the use of a mesh with the appropriate refinement level was encountered to have great significance in order to obtain the corresponding regime flow. The results of the simulations could be improved by incorporating a second refinement involving the velocity field, which is proposed as a future task.

ACKNOWLEDGEMENTS

This work has received financial support from Consejo Nacional de Investigaciones Científicas y Técnicas (CONICET, Argentina), Universidad Nacional del Comahue (UNCo, Argentina, grant 04/I-215), Agencia Nacional de Promoción Científica y Tecnológica (ANPCyT, Argentina, grant PICT-2014-2460), Universidad Tecnológica Nacional Facultad Regional del Neuquén (UTN FRN, Argentina), and was performed with the Free Software Foundation /GNU-Project resources such as GNU-LinuxOS and GNU-Doxygen, as well as other Open Source resources as L^AT_EX, OpenFOAM®, ParaView and Scilab.

REFERENCES

- Beggs D.H., Brill J.P., et al. A study of two-phase flow in inclined pipes. *Journal of Petroleum technology*, 25(05):607–617, 1973.
- Crowe C. *Multiphase Flow Handbook*. Mechanical and Aerospace Engineering Series. CRC Press, 2005. ISBN 9781420040470.
- Hänsch S., Lucas D., Höhne T., Krepper E., and Montoya G. Comparative simulations of free surface flows using vof-methods and a new approach for multi-scale interfacial structures. In *ASME 2013 Fluids Engineering Division Summer Meeting*, pages V01CT23A002–V01CT23A002. American Society of Mechanical Engineers, 2013.
- Izarra Labeaga J. and Herreras Omagogeascoa N. Two-phase pipeflow simulations with openfoam. 2013.
- Min L. *Experimental and computational study of two-phase slug flow*. Ph.D. thesis, Department of Chemical Engineering Imperial College London, 2015.
- Petalas N., Aziz K., et al. A mechanistic model for multiphase flow in pipes. *Journal of Canadian Petroleum Technology*, 39(06), 2000.
- Shuard A.M., Mahmud H.B., and King A.J. Comparison of two-phase pipe flow in openfoam with a mechanistic model. In *IOP Conference Series: Materials Science and Engineering*, volume 121, page 012018. IOP Publishing, 2016.
- Taitel Y. and Dukler A. A model for predicting flow regime transitions in horizontal and near horizontal gas-liquid flow. *AIChE Journal*, 22(1):47–55, 1976.
- Thaker J.P. and Banerjee J. Cfd simulation of two-phase flow phenomena in horizontal pipelines using openfoam. In *Proc. 40th Nat. Conf. on Fluid Mech. & Fluid Power*. 2013.
- Vershinin V.E., Ganopolsky R.M., and Polyakov V.O. Numerical modeling of two-dimensional

- gas-liquid flow structures. *Modern Applied Science*, 9(2):236, 2015.
- Wilcox D.C. *Turbulence Modeling for CFD*. DCW Industries, 2006.
- Yeoh G.H. and Tu J. *Computational Techniques for Multi-Phase Flows*. Butterworth-Heinemann, Elsevier Ltd., The Boulevard, Langford Lane, Kidlington, Oxford OX5 1GB, UK, first edition, 2010.